RSC Advances

ROYAL SOCIETY OF CHEMISTRY

PAPER

View Article Online
View Journal | View Issue

Cite this: *RSC Adv.*, 2026, **16**, 1546

Micellar extraction followed by flow injection ICP-AES for preconcentration and determination of aluminium ions

Shahab Shariati,*[a] Yadollah Yamini,[b] Mohammad Faraji,[c] Abolfazl Saleh[d] and Elahe Bozorgzadeh[a]

In this study, a convenient and sensitive off-line cloud point extraction method (off-line CPE) was developed to preconcentrate trace amounts of aluminium (Al) ions prior to their determination by flow injection (FI) coupled to inductively coupled plasma-atomic emission spectrometry (ICP-AES). The method is based on the formation of a complex between Al^{3+} and 3, 2′, 4′, 5, 7-penta hydroxy flavone reagent, using Triton X-114 as a non-ionic surfactant to extract the formed complex and facilitate phase separation. Following extraction, the micellar phase containing Al ions was analyzed using ICP-AES coupled with a flow injection system (FI-ICP-AES). The off-line CPE variables were optimized using the Taguchi method, resulting in optimal conditions of pH 4.5, 1000 μg L^{-1} reagent, 0.1% (w/v) Triton X-114, 0.25 mol L^{-1} salt concentration, and an equilibrium temperature of 60 °C. Under these conditions, a linear calibration range of 1.0–500 μg L^{-1} was achieved for determination of Al ions, with a detection limit (DL) of 0.89 μg L^{-1}, an enhancement factor of 54.7, and a relative standard deviation (RSD) below 3.1%. The accuracy and applicability of the proposed off-line CPE/FI-ICP-AES method were evaluated by analyzing Al ions in various aqueous samples, yielding satisfactory and reliable results.

Received 14th November 2025
Accepted 22nd December 2025

DOI: 10.1039/d5ra08800c

rsc.li/rsc-advances

1. Introduction

Aluminium (Al), the most abundant metal in the Earth's crust at approximately 8.8% by weight, is a pervasive environmental contaminant with extensive applications across various industries, including textiles, paper, food processing, electronics, cosmetics, and pharmaceuticals.[1–4] Despite its widespread use, aluminium poses significant ecological and human health risks due to its toxicity. In the environment, aluminium adversely affects aquatic ecosystems and impairs root development, thus limiting agricultural plant growth, particularly in acidic soils.[5,6] For human health, aluminium exposure has been linked to serious neurological disorders, including Alzheimer's disease and multiple sclerosis.[7] It can also adversely affect red blood cells,[8] parathyroid glands, and chromosomes.[9] Studies have suggested correlations between aluminium exposure and certain autism cases, supported by evidence of abnormal aluminium deposits in brain tissue.[10,11] Patients with impaired kidney function are at increased risk since they cannot efficiently eliminate the metal, potentially leading to neurotoxicity and other severe complications.[12,13] Consequently, elevated aluminium levels serve as a critical clinical indicator of potential central nervous system toxicity.[14] Other documented health effects include dialysis encephalopathy syndrome, Parkinson's disease,[15,16] and aluminium-induced bone disease from skeletal accumulation.[17–19]

Different preconcentration methods including cloud point extraction[20–25], coprecipitation,[23] and analytical methods such as sensors,[2,26–29] electrothermal atomic absorption spectrometry (ET-AAS),[30–32] spectrofluorimtery,[28,33–36] and inductively coupled plasma-atomic emission spectrometry (ICP-AES)[37] have been used for the determination of aluminum (Al^{3+}) ions. At low concentrations of Al^{3+} in real samples, suitable enrichment procedures are required for Al^{3+} determination. The capabilities of micellar systems and other self-assembled molecular assemblies have been acknowledged for a long time and have seen growing use in multiple domains of analytical chemistry recently. Cloud point extraction (CPE) relies on the use of high-concentration solutions of specific uncharged and zwitterionic surfactants, which form a uniform solution under certain environments. Water solubility of the surfactant decreases by altering temperature, pressure, or adding certain substances, causing the solution to become cloudy.[38–42]

Trace amounts of metals in complex matrices have been analysed using CPE methods, which present a practical

[a]*Department of Chemistry, Ra.C., Islamic Azad University, Rasht, Iran. E-mail: Sh. Shariaty@iau.ac.ir; Fax: +98-1313462231*

[b]*Department of Chemistry, Faculty of Sciences, Tarbiat Modares University, Tehran, Iran*

[c]*Food, Halal and Agricultural Products Research Group, Food Technology and Agricultural Products Research Center, Standard Research Institute (SRI), Karaj, Iran*

[d]*Iranian National Institute for Oceanography and Atmospheric Science (INIOAS), Tehran, Iran*

alternative to conventional extraction techniques,[43,44] that require large volumes of toxic and costly solvents. Such solvents pose significant risks to human health and the environment. In contrast, CPE methods are faster, safer, and more efficient, employing environmentally friendly surfactants that align with the principles of green analytical chemistry. For trace metal analyse, CPE is commonly adjusted to incorporate hydrophobic molecules through ligand complexation to enhance extraction efficiency. Upon heating, this mixture move into the cloud point phase, facilitating straightforward separation using centrifugation. When suitable chemicals and conditions are utilized, extraction at ambient temperature is reliable and effective, requiring only a brief period to finish.[30,38,45–49]

In this study, we combined off-line cloud point extraction with flow injection for sample introduction into the analytical instrument. A straightforward and adaptable system (off-line CPE/FI-ICP-AES) was developed to preconcentrate and determine Al ions in aqueous samples. During off-line CPE preconcentration, the hydrophobic chelate formed between Al^{3+} ions and 3, 2′, 4′, 5, 7-pentahydroxy flavone (morin) was extracted into the surfactant phase, which was subsequently injected into the FI-ICP-AES for further analysis.

The method novelty and enhanced analytical performance are achieved through a synergistic integration of three key components: morin as a selective chelating agent for Al^{3+}, Taguchi experimental design for systematic and robust multivariable optimization of the extraction process, and the off-line coupling of CPE with FI-ICP-AES for efficient analyte introduction. This triad directly addresses the principal constraints of CPE method for aluminum—namely, susceptibility to interferences from non-optimal chelation, inefficiencies from univariate optimization, and potential dilution or transfer losses. Consequently, the protocol delivers the superior analytical metrics including an expanded linear dynamic range and a significantly lowered detection limit, there by advancing the state-of-the-art in trace aluminum determination.

2. Experimental

2.1. Chemicals and reagents

All chemicals were used with analytical reagent grade. Al^{3+} stock solution (1000 mg L^{-1}) was prepared by directly dissolving aluminium nitrate (Merck; Darmstadt, Germany) in 0.1 M HNO_3. This standard solution was diluted with deionized water to prepare other concentrations of Al^{3+} ions. Reagent grade 3, 2′, 4′, 5, 7-pentahydroxy flavone ($C_{15}H_{10}O_7$; morin) obtained from Merck was utilized as chelating agent. The morin standard solution was prepared by dissolving an appropriate amount of the reagent in extra-pure methanol (Merck). Triton X-114, a non-ionic surfactant (Fluka, Chemie AG, Switzerland), was employed without further purification. A 2.5% w/v solution was prepared by dissolving 1.25 g of Triton X-114 in 50 mL of deionized water.

2.2. Instruments

An ICP-AES (Varian Vista-PRO, Australia) with a radial torch, a V-groove nebulizer, and a charge-coupled device (CCD), was applied to determine of Al^{3+} ions. Argon gas (99.999% purity) was sourced from Roham Gas Company (Tehran, Iran). To adjust the temperature of the solutions and to accelerate the phase separation in CPE process, a thermostat water bath (Khodsaz Company, Tehran, Iran) and a centrifuge (Ferdous Ray Company, Tehran, Iran) were utilized, respectively. A peristaltic pump (Farayand Gostar Company; Tehran, Iran) and a two-position injection valve (Tehran University, Iran) were used to deliver the sample in flow injection system (FI). Furthermore, a Heidolph MR 3001 K heater stirrer (Kelheim, Germany) and a pH meter (Inolab, Germany) were utilized for solution stirring and adjusting the pH of solutions, respectively.

2.3. Procedure of off-line CPE/FI-ICP-AES

In off-line CPE procedure, 10 mL of the solution containing Al^{3+} ions was adjusted to the appropriate salt concentration and pH (0.25 mol L^{-1} sodium acetate; pH = 4.5). Aluminium ions were complexed with the morin reagent. Subsequently, Triton X-114 (at 0.1% (w/v)) was added, and the solution was mixed thoroughly. The samples were then heated in a water bath at 60 °C for 15 min until turbidity appeared, indicating phase separation. The surfactant-rich micellar phase typically settled at the bottom of the aqueous phase and was collected for further analysis. To speed up phase separation in CPE, the mixtures were centrifuged at 4000 rpm for 10 min. Afterward, the tubes were placed in a freezing bath for 5 min to further densify the micelle-rich phase, facilitating easier separation of the aqueous phase by pipetting. Following the aqueous phase removal, a fixed volume of 150 μL of 50% (v/v) propanol in distilled water was added to the micelle-rich phase – obtained in off-line CPE – to reduce its viscosity. The surfactant-rich phase was then entered into the ICP-AES through flow injection *via* a six-port injection valve equipped with a homemade 160 μL loop positioned between ports 1 and 4 of the valve. The diluted surfactant-rich phase was loaded into the loop using a microsyringe while the valve was in the "load" position. Once loaded,

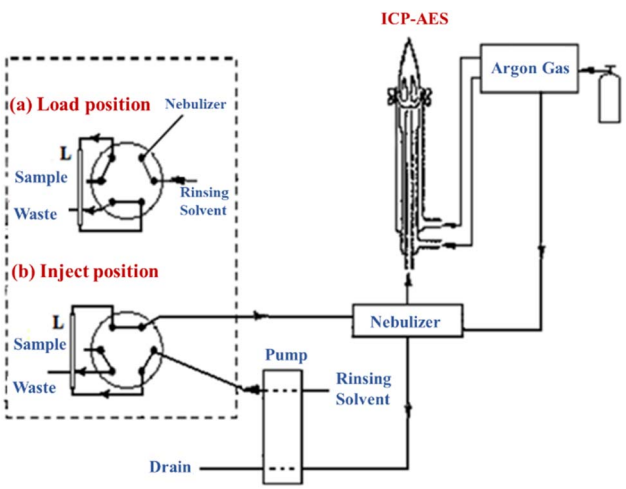

Fig. 1 Schematic diagram of the six-port injection valve containing loop (L) in conjugation of FI to ICP-AES. (a) Load position, and (b) inject position.

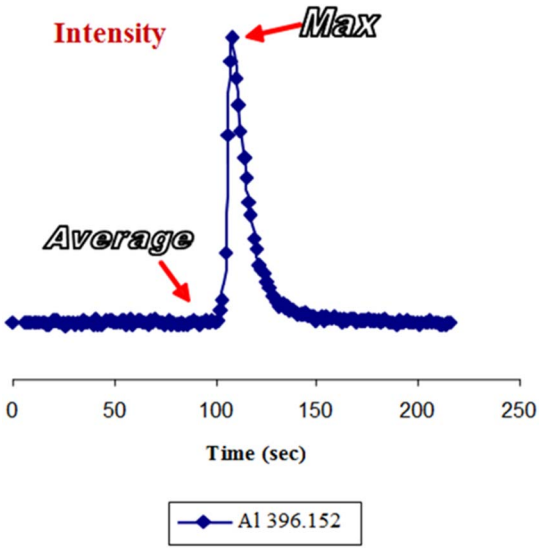

Fig. 2 Emission intensity measurement in time scan mode.

the valve was switched to the "inject" position, allowing the eluent to flow through the loop and rinse the analyte to the ICP-AES nebulizer, where the emission signal of Al was recorded over time. The emission intensity of Al at 396.152 nm was monitored, with corrections made using a blank solution for calibration. The schematic of the designed FI-ICP-AES system for Al^{3+} ion analysis after off-line CPE is presented in Fig. 1.

In FI-ICP-AES, the plasma was first activated during the sample loading step, with the injection valve set to the "load" position. Following several injection cycles, a cleaning solution was introduced into the loop to ensure thorough washing and purification. Using a Hamilton syringe, 180 μL of the surfactant-rich phase was injected into the six-port injection valve containing the loop to fill it completely. Subsequently, the valve was switched to the "inject" position, and the rinsing solution was pumped through the loop by a peristaltic pump. This process rinsed the sample through the loop into the nebulizer, enabling measurement of the Al emission at the appropriate wavelength during atomization. The instrument operated in time-scan mode, recording the emission intensity of Al at the specified wavelength during each injection as a function of time. The emission intensity was calculated as the difference between the peak intensity of the emission spectrum and its baseline value, as detailed in the following equation and Fig. 2.

$$\text{Peak height intensity} = \max(\text{all of points}) - \text{Average}_{(\text{baseline points at the left of the peak})}$$

3. Results and discussion

Morin (Fig. 3) is a phenolic compound derived from the substitution of hydroxyl groups on the flavone chromophore. It forms complexes with non-paramagnetic metal ions, particularly Al^{3+}.

Morin contains two active sites for chelation: the 3-hydroxy and 4-oxo sites, as well as the 5-hydroxy 4-oxo site. Additionally,

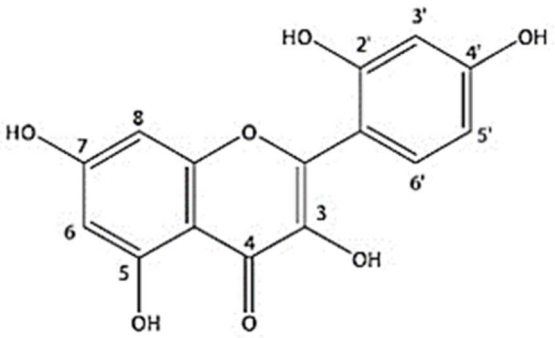

Fig. 3 Chemical structure of morin.

the 2,3 dihydroxy system can also act as a chelating agent, capable of forming a 7-membered chelate with Al^{3+}. Studies indicate that when measuring Al^{3+} through spectrophotometry and fluorimetry, an acetate medium with a pH of 3.5 to 6.5 is ideal for forming complexes.[50–52] The stoichiometric ratio of the Al-morin complex is influenced by the solvent used and the solution pH. In a methanol solution, Al^{3+} forms two types of complexes with morin at stoichiometries 1 : 1 and 1 : 2, while in acidic methanol solutions containing 0.1 mol L^{-1} nitric acid, only 1 : 1 complexes are formed. The absorption spectrum of morin exhibits a maximum peak at 355 nm, which decreases in intensity in aqueous solutions at pH 4.5 (using 0.05 mol L^{-1} ammonium acetate).[51,52] Increasing the concentration of Al^{3+} ions causes the absorption band of morin at 355 nm to diminish, while a new absorption band appears at 413 nm.[52] This red shift in the absorption spectrum of morin is attributed to the formation of a complex between Al^{3+} ions and morin, likely due to coordination of the lone pair of electrons on the oxygen donor atom with the Al^{3+} ion, resulting in reduced electron density on the chromophore. The stoichiometry of the complex formed between Al^{3+} and morin has been investigated using the molar ratio method in solutions with uncontrolled pH.[52] The molar ratio curve at a wavelength of 415 nm for uncontrolled pH exhibited an inflection point at an $Al^{3+}/M = 1.5$ ratio, indicating a stoichiometry of 3 : 2 (Al_3M_2) for the complex. While the molar ratio curves at wavelengths 355 and 413 nm at pH = 4.5 (amunium acaetate) exhibited an inflection point at an $Al^{3+}/M = 1$ ratio, indicating a stoichiometry of 1 : 1 (AlM) for the complex.[52]

3.1. Optimizing the FI-ICP-AES instrumental variables

Prior to analysing standards and samples, optimization was conducted to achieve the highest emission intensity for Al^{3+} ions. Various variables influencing the Al atomic emission signals in FI-ICP-AES were optimized using a univariate approach. For this purpose, a 5 mg L^{-1} Al^{3+} standard solution in 50% (v/v) propanol in distilled water containing 10% (w/v) Triton X-114 was prepared and directly introduced into the FI-ICP-AES system *via* six-port injection valve using a micro-syringe. Homemade loops with internal volumes of 100 and 160 μL were made for these optimizations. Instrumental variables including viewing height, nebulizer pressure, type and volume of the organic solvent (used to reduce viscosity of the surfactant-

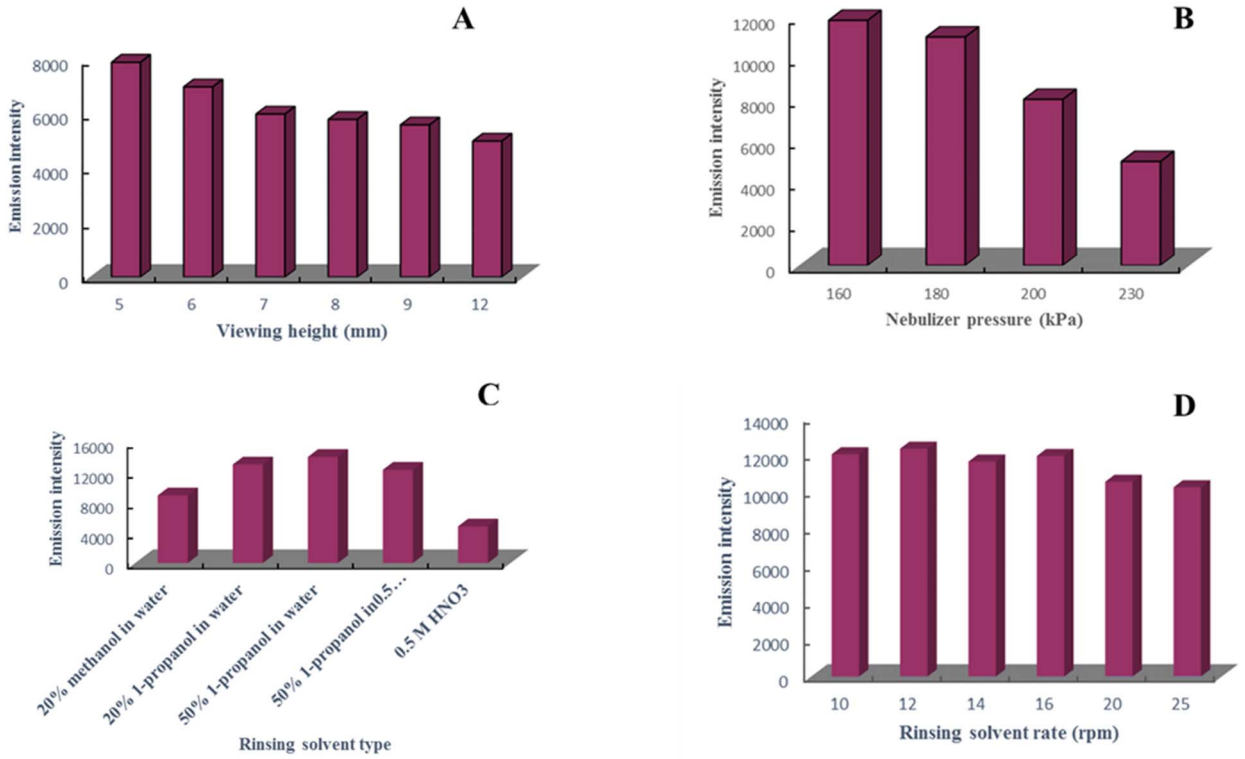

Fig. 4 Effects of instrumental variables including (A) viewing height (B) nebulizer pressure (C) rinsing solvent type, and (D) rinsing solvent rate on the Al emission intensity in ICP-AES.

rich phase), rinsing solvent flow rate and loop volume were investigated. The effects of each instrumental variable are illustrated in Fig. 4. Each level of studied variables was investigated at multiple replicate injections and the average of intensities were used.

The maximum emission intensity in the plasma, evaluated relative to the plasma height above the coil, can be affected by the element type, solvent, sample matrix, power supply, and nebulizer gas pressure. For optimizing the viewing height, argon gas was purged with a plasma gas flow rate of 15 L min^{-1}, an auxiliary flow rate of 1.5 L min^{-1}, and the RF generator operating at 40 MHz frequency. Fig. 4(A) illustrates the signal intensity as a function of time for a 10 mg L^{-1} Al^{3+} solution using the FI method, based on several consecutive injections at each viewing height. As observed, the highest emission intensity was recorded at the lower viewing height. Consequently, a height of 6 mm above the induction coil was selected as the optimal viewing height to achieve greater sensitivity and reproducibility. Fig. 5 shows the effect of viewing height for a 10 mg L^{-1} Al^{3+} solution analyzed using the FI method, based on multiple consecutive injections recorded in time-scan mode at each viewing height.

Nebulizer pressure influences signal intensity in two main ways. First, increasing nebulizer pressure enhances nebulization efficiency, allowing more analyte species to enter the plasma. However, higher pressure shortens the residence time of species within the plasma, potentially reducing their opportunity for excitation and emission. The optimal nebulizer pressure depends on factors such as viewing height, RF power, and sample flow rate. As shown in Fig. 4(B), at a viewing height of 6 mm, the signal intensity *versus* nebulizer pressure plot indicates 160 kPa as the optimal pressure value.

One of the most critical variables affecting the preconcentration process is the choice of solvent used to reduce the viscosity of the surfactant-rich phase and facilitate its rinsing from the loop. Even a small increase in the amount of organic solvents can disrupt micelle aggregates, thereby lowering the viscosity of the surfactant-rich phase. A selection of common organic solvents was investigated. To prevent baseline shifts in the injection system, it is ideal that the diluent for the surfactant-rich phase and the rinsing solvent of the loop to be of the same type; otherwise, baseline fluctuations may occur. Pure organic solvents, due to their high vapour pressure, can cause plasma quenching or instability, which compromises analytical performance. Therefore, mixtures of organic solvents with water were employed to balance these effects. Several diluents were evaluated, including 0.5 mol L^{-1} nitric acid, 20% (v/v) methanol in distilled water, 20% (v/v) 1-propanol in distilled water, 50% (v/v) 1-propanol in 0.5 mol L^{-1} nitric acid, and 50% (v/v) 1-propanol in distilled water. As indicated in Fig. 4(C), the 50% (v/v) 1-propanol in distilled water delivered the best performance and was selected as the optimal diluent for the system.

To investigate the flow rate of rinsing solvent from the loop, the rinsing solvent (50% (v/v) 1-propanol in distilled water) was

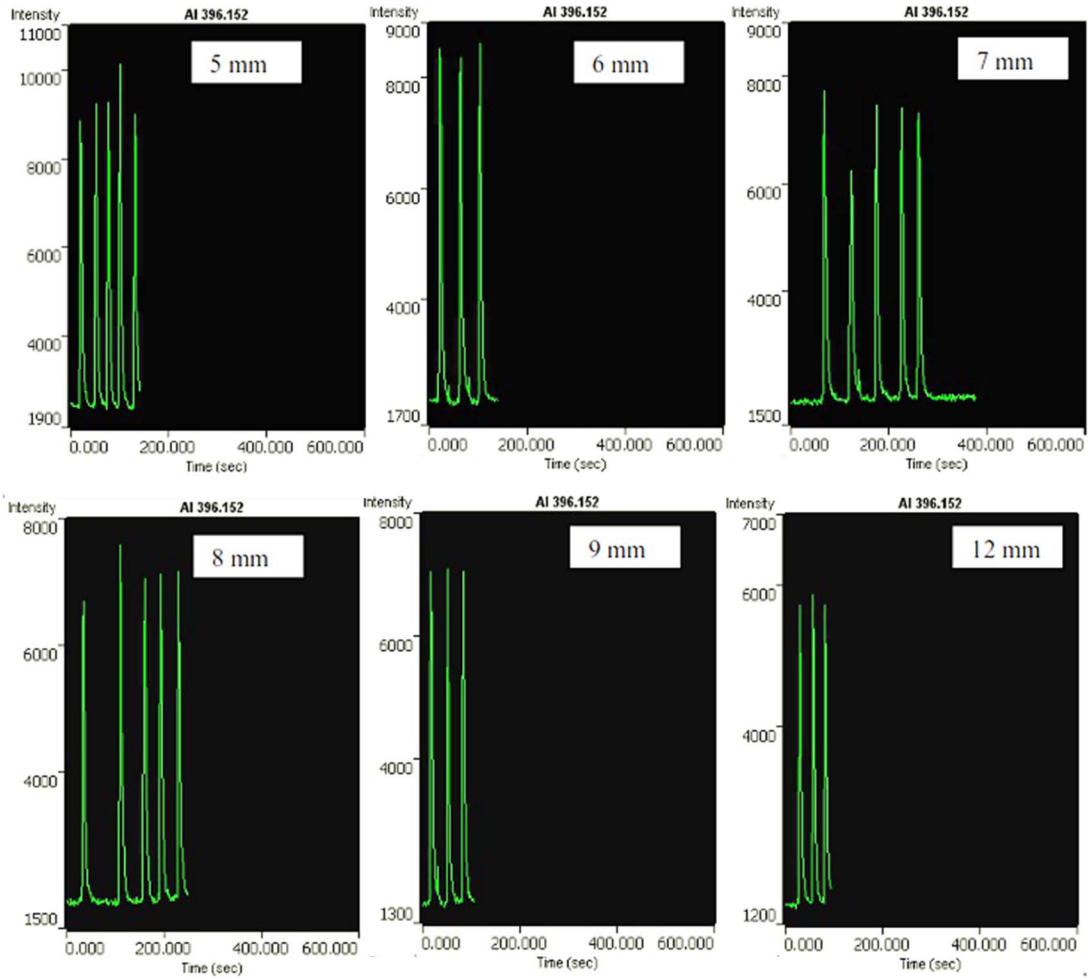

Fig. 5 Optimal viewing height design for a 10 mg L^{-1} Al^{3+} solution using the flow injection method, based on multiple consecutive injections at each viewing height.

circulated through the loop containing the sample using the peristaltic pump at different flow rates (viewing height = 6 mm, nebulizer pressure = 160 kPa). The emission intensity of Al was measured after three injections at each flow rate. As shown in Fig. 4(D), a flow rate of 12 rpm was identified as optimal. To investigate the effect of rinsing solvent and loop volume, loops with volumes of 100 and 160 μL were used. The volume of rinsing solvent was varied from 70 to 220 μL (70–130 μL for the 100 μL loop and 150–220 μL for the 160 μL-loop). The most stable condition was observed when the rinsing solvent completely filled the loop. Based on these results, the 160 μL loop was selected, and 150 μL of rinsing solvent was added to the surfactant-rich phase (resulting in a final volume after mixing with surfactant-rich phase in the range of 165–175 μL). The optimized ICP-AES instrumental parameters are summarized in Table 1.

3.2. Investigation of effective variables on the off-line CPE process

The variables affecting the off-line CPE efficiency, including surfactant and ligand concentrations, equilibrium temperature, pH, and ionic strength, were optimized using an orthogonal array (OA) optimization method to assess the significance of each variable on the extraction process. The OA_{25} design was employed to study five factors at five levels, aiming to identify the optimal CPE conditions. The parameters investigated included pH (4.0 to 7.0), surfactant concentration (0.05 to 0.4% w/v), ligand to metal (L/M) molar ratio (2 to 40), ionic strength (0.05 to 0.25 mol L^{-1}), and equilibrium temperature (30 to 70 °C in water bath). All experiments used 10 mL of Al^{3+} solution at 100 μg L^{-1}, with equilibrium and centrifuge times of 15 and 10 min, respectively. Each OA_{25} experimental trial was performed in duplicate, and average results were analyzed. The main effects of each variable on the emission intensity were calculated to determine the optimal conditions. Considering the number of factors, a total of 25 experiments were conducted in a randomized order to avoid bias. The experimental design and factor levels are detailed in Table S1 (SI).

Analysis of variance (ANOVA) was utilized to analyse the results and assess the contribution of each experimental parameter.[53] Key statistical metrics, including the *F*-ratio, sum of squares (SS), percent contribution (PC%), and purified sum of squares (SS′) for both error and experimental factors, were calculated and are presented in Table 2.

Table 1 The optimized conditions for ICP-AES determination of Al

RF generator power (kW)	1.65	Viewing height (mm)	6
Frequency of RF generator (MHz)	40	Pump rate (rpm)	12
Plasma gas flow rate (L min^{-1})	15.0	Al wavelength (nm)	396.162
Auxiliary gas flow rate (L min^{-1})	1.5	Loop volume (μl)	160
Nebulizer pressure (kPa)	160	Rinsing solvent	50% v/v of 1-propanol

The sum of squares of error (SS error) was calculated by subtracting the sum of squares of the factors from the total sum of squares. Based on the ANOVA results, the ligand-to-metal molar ratio (L/M; PC% = 74.09%) was identified as the most significant factor affecting the extraction of Al^{3+}, followed by surfactant concentration % (PC% = 7.99%), solution pH (PC% = 4.74%), solution temperature (PC% = 2.36%), and ionic strength (PC% = 0.61%). For each factor, the Fisher ratio (F), was determined by dividing the variance of the factor by the variance of the error. The critical F-value ($F_{critical}(4,29)$) was 2.70 at a significance level of $P = 0.05$. Comparing the calculated F-values in Table S1 with $F_{critical}$, indicated that pH ($F = 6.08$), surfactant concentration ($F = 9.56$), temperature ($F = 3.53$) and L/M molar ratio ($F = 80.40$) significantly influenced the extraction process as their F-values exceeded the critical value (F-values > $F_{critical}$).

In the extraction of metal ions by CPE method, a hydrophobic complex is first formed and then extracted into a reduced volume of micelles to achieve preconcentration. The efficiency of this extraction process depends on the pH at which complex formation occurs. In this research, the effect of solution pH on complex formation was evaluated in the pH range of 4.0 to 7.0 using a sodium acetate solution, along with NaOH or HNO_3. As shown in Fig. 6, the emission intensity reached its maximum at pH 4.5. Therefore, pH 4.5 was selected for the following extraction steps.

The salt effect was investigated by adding sodium acetate to the solution, in the concentrations ranging from 0.05 to 0.75 mol L^{-1}. Similar extraction results were achieved with sodium acetate concentrations of 0.25 to 0.5 mol L^{-1}. Consequently, 0.25 mol L^{-1} was chosen as the optimum value for further experiments (Fig. 6).

Triton X-114 was selected because of its commercial availability in a highly purified and homogeneous form, low toxicity, and cost-effectiveness, low cloud point temperature and dense micelle-rich phase, making it a suitable surfactant for CPE.

The effect of surfactant concentration on the extraction efficiency was examined within the Triton X-114 concentration range of 0.05 to 0.4% w/v. As observed in Fig. 6, quantitative extraction was achieved at 0.1% w/v. Lower surfactant concentrations led to reduced extraction efficiency, likely due to insufficient aggregate formation to effectively capture the formed complex. Conversely, at concentrations above 0.1% w/v, a decrease in emission intensity was observed, which can be attributed to the increased volume of the micelle-rich phase. Therefore, 0.1% w/v Triton X-114 was selected as the optimal concentration to ensure high extraction efficiency and effective enrichment factor.

The stoichiometric ratio of Al : morin complexes is influenced by factors such as the solvent and solution pH. Specifically, at pH 4.5, a 1 : 1 stoichiometric complex (AlM) is formed. The relationship between emission intensity and reagent concentration was studied by altering the molar ratio of morin to Al from 2 to 40. The findings indicated that a morin to Al molar ratio of 40 yielded the highest extraction efficiency. Consequently, this ratio was chosen as the optimal ligand-to-metal (L/M) ratio. Fig. 6 illustrates the variation of extraction efficiency with different L/M molar ratio.

Employing the lowest possible equilibration temperature is desirable to balance effective complexation with efficient phase separation. With increasing equilibration temperatures, the phase volume of non-ionic surfactants typically diminishes. Consequently, optimal analyte preconcentration during CPE is achieved at temperatures significantly above the surfactant's cloud point temperature (CPT).

The phase separation temperature is influenced by surfactant concentration and can be modified by the addition of other substances such as salts, ligand, *etc.* It was determined that 60 °C is adequate for complex extraction, and thus was selected for further experiments. Fig. 6 displays how extraction efficiency varies with equilibration temperature.

Table 2 ANOVA results for Taguchi experimental design in the OA_{25} matrix

Factor	DF[a]	SS[b]	MS[c]	F-ratio[d]	SS′[e]	PC[f] (%)
pH	4	784 150 115	196 125 28.8	6.08	655 386 236	4.47
Surfactant	4	123 495 7213	308 739 303	9.56	1 105 842 299	7.99
Ionic strength	4	4 509 692	11 274 229	0.35	−84 017 999	0.61
Temperature	4	45 618 069.89	114 045 175	3.53	327 065 785	2.36
L/M	4	1 038 079 580	2 595 198 949	80.40	1 025 168 088	74.09
Error	29	9 360 831 261	3 227 872.9		158 165 770	11.43
Total	49	1 383 761 490				

[a] DF: degree of freedom; DF for each parameter = number of levels of each parameter − 1; DF for total results = number of total results − 1; DF for error = DF for total results − $\sum_f$ DF for each parameter. [b] SS: sum of squares. [c] MS: mean squares. [d] F-ratio: $F_{(4,29)}$, critical value is 2.70 ($P < 0.05$). [e] SS′: purified sum of squares. [f] PC (%): percentage contribution.

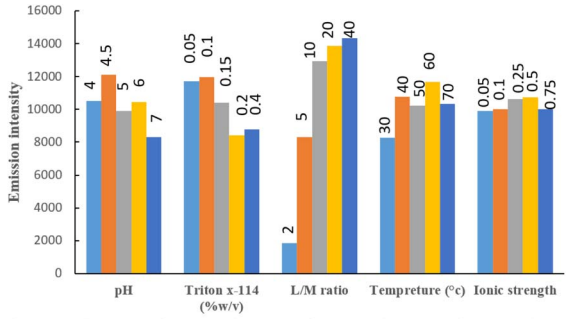

Fig. 6 Effect of experimental factors investigated by Taguchi method (the levels of each factor were added to the top of the column).

Based on the results of repetitive extraction experiments following the OA_{25} design, the optimum conditions of off-line CPE variables were pH 4.5, a *L*/*M* molar ratio of 40, 0.1% (w/v) Triton X-114, 0.25 mol L^{-1} salt concentration, and an equilibrium temperature of 60 °C. To investigate the precision of the proposed off-line CPE/FI-ICP-AES method for Al^{3+} analysis, five replicate extractions were performed on 10 mL solutions containing 100 μg L^{-1} Al^{3+} under optimum conditions. The empirical mean emission intensity after five repetitive extractions was 14 524.4 ± 853.74 (standard deviation), which agrees well with the Taguchi method-predicted value of 14 334.41 ± 1161.99.

3.3. Study the effect of potential interferences on the off-line CPE/FI-ICP-AES of Al^{3+} ions

Due to the high selectivity of ICP-AES, the investigation focused solely on ions capable of forming complexes with Al^{3+} or morin reagent, which could potentially affect Al^{3+} preconcentration by off-line CPE. Various ions likely to be present in real samples were examined as potential interfering species. To study the interference effects, separate 10 mL solutions containing 100 μg L^{-1} Al^{3+} and different foreign ions at interference to Al^{3+} concentration ratios ranging from 5 to 2000 were processed using the proposed extraction method. The interference effect was assessed by comparing the Al emission intensity in the presence and absence of these foreign ions, with a ±10% deviation considered indicative of interference. The effects of interfering ions are summarized in Table 3.

The outcomes demonstrated that Na^+ and K^+ ions (at 150 mg L^{-1}), alkaline earth ions, Ni^{2+}, Pb^{2+}, Zn^{2+} and Co^{2+} ions (at 100 mg L^{-1}), as well as Mn^{2+} ions (at 50 mg L^{-1}), showed no interference effect on Al analysis by the proposed method. However, certain ions, including Fe^{3+}, Cu^{2+}, Hg^{2+}, and F^- caused interference in the CPE of Al^{3+} under the specified conditions. Further experiments revealed that Fe^{3+} ions at a concentration of 5 mg L^{-1} produced severe interfering effect on the Al analysis. By reducing Fe^{3+} concentration to 0.5 mg L^{-1} and addition of 0.02 mol per L thiocyanate (SCN^-) to the sample, this interference is resolved. This effect is likely due to the possible reaction of Fe^{3+} and SCN^- ions forming $Fe(SCN)_x^{3-x}$. Interference from Cu^{2+} at 5 mg L^{-1} (50 times the Al^{3+} concentration) was completely eliminated by the addition of 0.01 mol per L ascorbic acid and KI. Ascorbic acid reduced Cu^{2+} to Cu^+, which then reacts with I^- to form CuI_2^- complex, thus resolving Cu^{2+} interference. Similarly, Hg^{2+} interference was completely removed by adding 0.01 mol per L KI, resulting in the formation of HgI_2. In solution, F^- ions react with Al^{3+} to

Table 3 Effects of possible interfering ions on the recovery of 100 μg L^{-1} of Al^{3+}

Ion	Concentration (mg L^{-1})	C_x/C_{Al}	Recovery (%)
Na^+, K^+	200	2000	116.8
	150	1500	100.6
Alkaline	200	200	131.3
Earth metal metals	150	1500	113.4
	100	1000	97.24
Ni^{2+}	100	1000	101.2
Mg^{2+}	100	1000	120.2
	50	500	93.9
Pb^{2+}	100	1000	103.4
Zn^{2+}	100	1000	98.9
Co^{2+}	100	1000	97.2
F^-	5	50	56.6
	0.5	5	98.9
Cd^{2+}	50	500	100.8
Fe^{3+}	5	50	HI[a]
	5	50 (0.01 mol L^{-1} SCN^-)	HI
	0.5	5 (0.02 mol L^{-1} SCN^-)	91.6
Hg^{2+}	5	50	81.4
	0.5	5	85.8
	50 (0.01 mol L^{-1} KI)	50	101.8
Cu^{2+}	10	100	Highly interferent
	5	50	65.4
	5 (0.02 mol L^{-1} SCN^-)	50	76.1
	5 (0.01 mol L^{-1} ascorbic + 0.01 mol L^{-1}) KI) acid + 0.01 M KI)	50	97.9

[a] Highly interferent.

Table 4 Comparison of the figures of merit of the proposed method with some other published methods for Al^{3+} determination

Analytical technique	LOD (μg L^{-1})	RSD (%)	LDR (μg L^{-1})	Ref.
CDots-FIA-fluorescent sensors	7.0	<13	40–3000	10
Spectrophotometry	0.01	—	0.01–800	54
CDs@ZIF-90-fluorescent sensors	21.87	—	27–5400	33
Fluorimetry	1.3	0.8	50–200	55
UA-DLLME-FI-fluorimetry[a]	1.7	0.95	11–180	56
Spectrofluorimetry	2.7	< 5	2.7–300	57
SPE-FAAS[b]	6.8	0.4–1.9	23–5000	58
Fluorimetry	68	—	1000–8000	59
Reflectance spectroscopy	3000	<5.0	10 000–125000	60
FI-BSI-spectrophotometry[c]	2	0.8–1.3	7.5–625	61
Stripping voltammetry	2.3	1.9	2.3–6.3	62
DSFME-spectrophotometry	0.09	2–4	0.28–500	63
Off-line CPE/FIA-ICP-AES	0.89	3.1	1.0–500	This study

[a] Ultrasound assisted dispersive liquid–liquid microextraction-flow injection. [b] Flame atomic absorption spectroscopy. [c] Flow-batch sequential injection system.

form a soluble AlF_6^{3-} complex, which reduces the amount of free Al^{3+} available for complexation with morin. Reducing F^- concentration to 0.5 mg L^{-1}, eliminated interference, and this concentration is logical for tap and surface water samples that usually have F^- levels below this value. F^- concentrations in standard drinking and bottled waters usually do not exceed this value. For matrices with inherently higher fluoride content, such as seawater or certain ground waters, the routine dilution performed prior to ICP-AES measurement sufficiently lowers the fluoride concentration to eliminate interference, thereby guaranteeing reliable aluminum quantification in diverse aqueous environments.

A summary of these results is provided in Table 3.

3.4. Analytical characteristics of the proposed off-line CPE/FI-ICP-AES

A calibration curve was prepared with 10 mL of standard solutions adjusted to pH 4.5, containing 0.1% (w/v) Triton X-114 and Al^{3+} concentrations varying from 1.0 to 500 μg L^{-1}. Each standard solution was subjected to extraction following the optimized off-line CPE/FI-ICP-AES procedure. The calibration curve was constructed by plotting the emission intensity against the Al^{3+} concentration in the aqueous phase. The calibration curves exhibited excellent linearity over the Al^{3+} concentration range of 1.0–500 μg L^{-1}, with a correlation coefficient (R^2) of 0.9977 ($I = 146.72C + 302.16$; where I and C represent emission intensity and concentration in μg L^{-1}, respectively) and a limit of detection (LOD) of 0.89 μg L^{-1}. The relative standard deviations (RSD (%)), as a measure of repeatability of the proposed off-line CPE/FI-ICP-AES method, for five replicates of 10 and 100 μg L^{-1} Al^{3+} were 3.1% and 2.8%, respectively. The direct calibration curve was plotted by analysing Al^{3+} solutions in the range of 1.0 to 50.0 mg L^{-1} using FI-ICP-AES. Also, to obtain greater enhancement factor (EF), off-line CPE procedures from 50 mL sample solutions were performed under the optimal conditions. In 50 mL solution, the calibration curve showed very good linearity over the Al^{3+} concentration ranging from 0.5–950 μg L^{-1}, with a correlation coefficient (R^2) of 0.9980 ($I = 440.21C -$ 695.8). The enhancement factors (EF), defined as the slope of the calibration curves after preconcentration to those obtained without preconcentration, were calculated as 54.7 and 153.8 for sample volumes of 10 and 50 mL, respectively.

3.5. Comparison of proposed method with other previously methods

The proposed method was compared with previously reported analytical techniques for the determination of Al^{3+}, as summarized in Table 4. The results reveal that the proposed method offers superior sensitivity, a broader linear dynamic range, and precision comparable to existing methods.

3.6. Application of the proposed off-line CPE/FI-ICP-AES for Al determination in real samples

To validate the applicability of the proposed off-line CPE/FI-ICP-AES method for extracting and measuring Al ions in water samples, various aqueous matrices were evaluated. Each sample was initially extracted following the addition of 0.02 mol per L SCN^- under the optimal conditions, and the Al concentration was determined. To assess matrix effects on extraction performance, the samples were spiked with 10 μg L^{-1} of Al^{3+} ions. Following spiking, the samples underwent extraction using off-line CPE procedure, and Al concentrations were quantified using a calibration curve derived from aqueous standards subjected to the same CPE process. The obtained results (Table 5) demonstrate strong agreement with the target values, confirming the method's suitability for the analysis of Al^{3+} ions in aqueous samples.

Table 5 Measurement of Al^{3+} ions by suggested off-line CPE/FI-ICP-AES in real samples

Sample	Mineral water	Tap water	Sea water
Determined (μg L^{-1})	3.4 ± 0.6	9.6 ± 1.6	9.5 ± 0.5
Spiked (μg L^{-1})	10	10	10
Found (μg L^{-1})	12.7 ± 1.4	20.4 ± 0.9	18.5 ± 1.1
Relative recovery	94.8	104.1	94.9

4. Conclusions

The application of micellar systems offers several advantages over traditional separation and preconcentration techniques, including ease of operation, enhanced safety, and cost-effectiveness. Compared to solvent extraction methods, micellar systems are much safer since they require only a small quantity of a low-toxicity surfactant. In this study, off-line CPE was employed to preconcentrate Al^{3+} ions prior to their quantification by FI-ICP-AES. This approach demonstrated a low LOD, satisfactory RSD (%) and excellent linearity for Al^{3+} ions. Validation with real water samples yielded satisfactory outcomes, affirming the method's applicability. Furthermore, results indicated that improved LODs and PFs could be achieved by processing larger sample volumes, enhancing sensitivity and analytical performance.

Author contributions

S. Shariati: investigation, conceptualization, methodology, formal analysis, visualization, software, resources, data curation, validation, writing – reviewing and editing Y. Yamini: investigation, conceptualization, methodology, funding acquisition, visualization, resources, reviewing and editing, M. Faraji & A. Saleh: methodology, formal analysis, visualization, resources, data curation, validation, visualization, E. Bozorgzadeh: validation, visualization, writing – reviewing and editing.

Conflicts of interest

There are no conflicts to declare.

Data availability

All data supporting the findings of this study are available within the Manuscript and its supplementary information (SI). No additional datasets were generated or analysed during this study. Supplementary information: Table S1: the OA_{25} Taguchi design for the optimization of experimental parameters in off-line CPE/FI-ICP-AES. See DOI: https://doi.org/10.1039/d5ra08800c.

Acknowledgements

The authors are grateful to Tarbiat Modares University for support of this research.

References

1 R. H. Alasfar and R. J. Isaifan, *Environ. Sci. Pollut. Res.*, 2021, **28**, 44587–44597.
2 N. Apiratikul, P. Bunrit, S. Jommaroeng, P. Boonsri and K. Songsrirote, *Sens. Int.*, 2025, **6**, 100313.
3 A. Mahmud-Ali, C. Fitz-Binder and T. Bechtold, *Dyes Pigm.*, 2012, **94**, 533–540.
4 A. Rouis, M. Echabaane, S. Khlifi and I. Bonnamour, *Int. J. Electrochem. Sci.*, 2025, **20**, 100890.
5 S. Al-Kindy, F. Suliman and S. Salama, *Microchem. J.*, 2003, **74**, 173–179.
6 A. Morita, H. Horie, Y. Fujii, S. Takatsu, N. Watanabe, A. Yagi and H. Yokota, *Phytochemistry*, 2004, **65**, 2775–2780.
7 T. P. Flaten, *Brain Res. Bull.*, 2001, **55**, 187–196.
8 L. Sombra, M. Luconi, M. F. Silva, R. A. Olsina and L. Fernandez, *Analyst*, 2001, **126**, 1172–1176.
9 B. Gammelgaard and E. Sandberg, *J. Trace Elem. Electrolytes Health Dis.*, 1989, **3**, 39–42.
10 D. Uriarte, N. Gómez, A. Canals, C. Domini and M. Garrido, *Talanta Open*, 2023, **7**, 100192.
11 C. Exley and E. Clarkson, *Sci. Rep.*, 2020, **10**, 7770.
12 P. D. Darbre, *J. Inorg. Biochem.*, 2005, **99**, 1912–1919.
13 O. Barbier, G. Jacquillet, M. Tauc, M. Cougnon and P. Poujeol, *Nephron Physiology*, 2005, **99**, p105–p110.
14 R. Williams, *Coord. Chem. Rev.*, 2002, **228**, 93–96.
15 M. Rogers and D. G. Simon, *Age and ageing*, 1999, **28**, 205–209.
16 T. P. Flaten, *Environ. Geochem. Health*, 1990, **12**, 152–167.
17 W. G. Goodman, in:*Aluminum and Renal Failure*, Springer, 1990, pp. 87–108.
18 L. D. Quarles, G. Murphy, J. B. Vogler and M. K. Drezner, *J. Bone Miner. Res.*, 1990, **5**, 625–635.
19 J. Savory, R. L. Bertholf and M. Wills, *Acta Pharmacol. Toxicol.*, 1986, **59**, 282–288.
20 S. Khan, T. G. Kazi, N. F. Kolachi, J. A. Baig, H. I. Afridi and F. Shah, *Desalination*, 2011, **281**, 215–220.
21 S. Khan, T. G. Kazi, J. A. Baig, N. F. Kolachi, H. I. Afridi, A. Q. Shah, G. A. Kandhro and S. Kumar, *Talanta*, 2009, **80**, 158–162.
22 H. İ. Ulusoy, R. Gürkan, Ü. Aksoy and M. Akçay, *Microchem. J.*, 2011, **99**, 76–81.
23 V. N. Bulut, D. Arslan, D. Ozdes, M. Soylak and M. Tufekci, *J. Hazard. Mater.*, 2010, **182**, 331–336.
24 S. Hongbo, L. Pei and D. Dan, *J. Hazard. Mater.*, 2008, **154**.
25 A. B. Tabrizi, *Food Chem.*, 2007, **100**, 1698–1703.
26 N. Goswami, S. Naithani, T. Goswami, P. Kumar and S. Kumar, *Spectrochim. Acta, Part A*, 2024, **310**, 123971.
27 G. M. Ziarani, F. Moradi-Chaleshtori, M. Mirhosseyni, M. Feizi-Dehnayebi and A. Badiei, *J. Mol. Struct.*, 2025, **1325**, 140947.
28 H.-Y. Niu, Y. Gao, X.-X. Li and W.-K. Dong, *J. Mol. Struct.*, 2024, **1305**, 137795.
29 F. Mollaamin and M. Monajjemi, *Comput. Theor. Chem.*, 2024, **1237**, 114646.
30 N. M. Abdulhussein, N. M. Muslim, M. A. Hussien, E. A. Azooz and E. A. J. Al-Mulla, *J. Iran. Chem. Soc.*, 2024, **21**, 1203–1212.
31 R. Mariychuk, S. Sukharev, O. Sukhareva, L. Roman and T. Babilia, *Environ. Geochem. Health*, 2024, **46**, 444.
32 K. Chovancová, N. M. Michalides, M. Košlabová, M. Končálová and R. Halko, *Anal. Methods*, 2024, **16**, 990–1002.
33 L. Peng, H. Guo, N. Wu, M. Wang, Y. Hao, B. Ren, Y. Hui, H. Ren and W. Yang, *Anal. Chim. Acta*, 2024, **1288**, 342171.
34 R. Zhao, W. Lu, X. Chai, C. Dong, S. Shuang and Y. Guo, *Anal. Chim. Acta*, 2024, **1298**, 342403.

35 K. Jian, L. Fu, Y. Zhang, H. Zhang, X. Guo and X. Zhao, *Int. J. Biol. Macromol.*, 2024, **260**, 129413.
36 T. J. Dathees, G. Narmatha, G. Prabakaran, S. Seenithurai, J.-D. Chai, R. S. Kumar, J. Prabhu and R. Nandhakumar, *Food Chem.*, 2024, **441**, 138362.
37 N. S. Mdluli, C. D. Knottenbelt, P. N. Nomngongo and N. Mketo, *Sci. Rep.*, 2024, **14**, 2362.
38 L. Tavakoli, Y. Yamini, H. Ebrahimzadeh, A. Nezhadali, S. Shariati and F. Nourmohammadian, *J. Hazard. Mater.*, 2008, **152**, 737–743.
39 M. F. Silva, E. S. Cerutti and L. D. Martinez, *Microchim. Acta*, 2006, **155**, 349–364.
40 H. Watanabe and H. Tanaka, *Talanta*, 1978, **25**, 585–589.
41 M. Ghambarian, Y. Yamini, A. Saleh, S. Shariati and N. Yazdanfar, *Talanta*, 2009, **78**, 970–976.
42 S. Shariati and M. Golshekan, *J. Anal. Chem.*, 2014, **69**, 248–254.
43 M. Faraji, Y. Yamini and S. Shariati, *J. Hazard. Mater.*, 2009, **166**, 1383–1388.
44 S. Shariati, Y. Yamini, M. Faraji and A. Saleh, *Microchim. Acta*, 2009, **165**, 65–72.
45 Y. O. Mussa, A. A. Ghali and A. S. Hussei, *Indian J. Forensic Med. Toxicol.*, 2020, **14**, 631–639.
46 S. Shariati and Y. Yamini, *J. Colloid Interface Sci.*, 2006, **298**, 419–425.
47 S. Shariati, Y. Yamini and M. K. Zanjani, *J. Hazard. Mater.*, 2008, **156**, 583–590.
48 Y. Yamini, M. Faraji, S. Shariati, R. Hassani and M. Ghambarian, *Anal. Chim. Acta*, 2008, **612**, 144–151.
49 E. A. AbdulKareem, A. Y. Al-Murshedi, R. K. Ridha and E. A. Azooz, *Green Anal. Chem.*, 2024, **11**, 100181.
50 Y. Feng, M. Shibukawa and K. Oguma, *J. Chromatogr. Sci.*, 1996, **34**, 425–430.
51 A. C. Gutierrez and M. H. Gehlen, *Spectrochim. Acta, Part A*, 2002, **58**, 83–89.
52 C. Septhum, V. Rattanaphani and S. Rattanaphani, *Suranaree J. Sci. Technol.*, 2007, **14**, 91–97.
53 R. Kouchakinejad, S. Shariati, J. Abolhasani, E. G. Kalhor and M. T. Vardini, *Colloids Surf., A*, 2022, **643**, 128709.
54 F. Hossain, S. Begum, I. Jahan and M. J. Ahmed, *Anal. Sci.*, 2020, **36**, 813–819.
55 Z.-y. Yuan, T.-y. Li, J.-f. Zhang and X.-m. Wang, *J. Hazard. Mater.*, 2022, **433**, 128815.
56 N. A. Gomez, A. S. Lorenzetti, J. Camiña, M. Garrido and C. E. Domini, *Microchem. J.*, 2022, **183**, 108117.
57 J. A. López-López, C. Borrego-Corchado, M. P. Mánuel and E. Espada-Bellido, *Talanta*, 2018, **182**, 210–217.
58 J. A. Sweileh, K. Y. Misef, A. H. El-Sheikh and M. S. Sunjuk, *J. Food Compos. Anal.*, 2014, **33**, 6–13.
59 F. H. Abdullah, N. A. A. Latif, F. B. M. Suah and F. S. Mehamod, *J. Lumin.*, 2017, **188**, 267–274.
60 A. L. P. Silvestre, M. I. Milani, E. L. Rossini, L. Pezza and H. R. Pezza, *Spectrochim. Acta, Part A*, 2018, **204**, 432–435.
61 Y. Khanhuathon, W. Siriangkhawut, P. Chantiratikul and K. Grudpan, *J. Food Compos. Anal.*, 2015, **41**, 45–53.
62 L. B. Santos, M. T. de Souza, A. T. Paulino, E. E. Garcia, E. M. Nogami, J. C. Garcia and N. E. de Souza, *Microchem. J.*, 2014, **112**, 50–55.
63 B. A. Alyami, A. M. Mahmoud, S. A. Alkahtani and M. M. El-Wekil, *Talanta*, 2021, **226**, 122167.